

This is the accepted manuscript made available via CHORUS. The article has been published as:

Effect of symmetry breaking on the optical absorption of semiconductor nanoparticles

Adam Gali, Efthimios Kaxiras, Gergely T. Zimanyi, and Sheng Meng

Phys. Rev. B **84**, 035325 — Published 29 July 2011

DOI: [10.1103/PhysRevB.84.035325](https://doi.org/10.1103/PhysRevB.84.035325)

Effects of symmetry breaking on optical absorption of semiconductor nanoparticles

Adam Gali*

*Research Institute for Solid State Physics and Optics,
Hungarian Academy of Sciences, Budapest, P.O.B. 49, H-1525 and
Department of Atomic Physics, Budapest University of Technology and Economics, Budafoki út 8., H-1111, Budapest, Hungary*

Efthimios Kaxiras

*Department of Physics and School of Engineering and Applied Sciences,
Harvard University, Cambridge MA 02138, USA*

Gergely T. Zimanyi

Physics Department, University of California, Davis, CA 95616, USA

Sheng Meng[†]

*Beijing National Laboratory for Condensed Matter Physics,
and Institute of Physics, Chinese Academy of Sciences, Beijing 100190, China*

The shape of semiconductor nanoparticles (NPs) can have an important influence on their optical absorption spectra, with enhanced absorption resulting from breaking their symmetry. To illustrate this effect, we present broad energy optical excitation spectra of ~ 2 nm Si and PbSe nanoparticles, obtained from extensive time-dependent density functional theory calculations. We considered both highly symmetric spherical shapes and low-symmetry rod-like and disc-like shapes. The low-symmetry shapes exhibit an increase in absorption at low and relatively high energies compared to the absorption of the spherical NPs of similar volume, independent of their chemical composition and surface structure. Our results elucidate the mechanism of enhanced Multi-Exciton-Generation in semiconductor NPs which is important in the quest to improve their photovoltaic applications.

PACS numbers: 78.67.Bf, 73.22.-f, 71.15.Qe

I. INTRODUCTION

In the quest for more efficient photovoltaic (PV) devices, the development of new materials and processes can play a crucial role. In particular, systems that can take advantage of the physics of nanoscale structures may open new possibilities and lead to breakthroughs in solar energy harvesting and conversion¹. An exciting possibility is the generation of more than one electron-hole pairs by each photon absorbed, a process referred to as “multi-exciton generation” (MEG), which has been observed in semiconductor nanoparticles (NPs)^{2,3,3–10}; this would increase the current and useful power output. MEG could actually be enhanced in NPs relative to the bulk material, which would further improve device efficiency. The physics behind this enhancement is the suppression of exciton decay by phonon emission in NPs (the “phonon bottleneck”) due to the reduced number of available vibrational states, and the more facile creation of additional excitons due to stronger Coulomb interaction in NPs from less efficient screening. Recent studies on II-VI and III-V NPs found that MEG efficiencies are smaller than originally suggested^{11–17}, and depend on surface chemistry, NP concentration, and measurement conditions that can lead to charging^{18–23}. While the degree of enhancement is debated by these papers, all of them agree that MEG *does* occur in PbSe^{14,17,23}.

Energy conservation implies that MEG can only be induced by an incident photon with energy $h\nu \geq mE_g$, where E_g is the optical gap and m an integer ≥ 2 . Bi-exciton creation ($m = 2$) is considered the optimal scenario for PV applications because the exciton lifetime decreases with increasing m ⁴ and the extraction of multiple excitons is challenging²⁴. Moreover, typical semiconductor band-gaps are in the range of 1 eV and the solar spectrum intensity peaks in the range 1.4–3.0 eV, making MEG with $m = 2$ or 3 the only practically relevant cases. For higher efficiency in solar energy conversion, the threshold energy for biexciton creation, E_{thr} , should be as close to the theoretical limit of $2E_g$ as possible, but it is larger in experiments⁴. The ratio E_{thr}/E_g depends on the material, the size and the surface of the NPs. Intriguingly, with decreasing NP size this ratio can be reduced: for instance, it is about 4.2 in the bulk and 2.7 in NPs of PbSe²⁵. Effects that increase the value of this ratio in bulk processes are the curvature of the band structure, the splitting of energy levels close to E_g , indirect transitions, and selection rules for optical excitation which are imposed by translational symmetry; the relaxation of selection rules in NPs can help bring this ratio closer to the desired limit²⁵. On the other hand, the finite size of NPs leads to quantum confinement and consequently larger E_g compared to the bulk. This can have an effect opposite to the trends mentioned so far: for instance, the number of excitons created by a photon at a specific excitation energy is larger in bulk than in NPs of PbSe^{26,27}, due to quantum-confinement-induced lower density of states in the NPs at the given excitation energy. A thorough

understanding of the physics behind these effects is the key to improving MEG in NPs, and to exploiting materials which otherwise may appear as unsuitable for PV applications from their bulk properties.

In this work we show through extensive first-principles calculations of optical properties that taking advantage of the symmetry of NPs can prove very effective in addressing some of the issues raised above. Semiconductors typically exhibit O_h symmetry in the bulk, which is reduced to T_d in NPs of spherical shape. The T_d group, one of the highest symmetry among the 3D crystallographic point groups, leads to a large number of selection rules with many dipole transitions forbidden to first order. Thus, in highly symmetric NPs, crystal momentum selection rules may not be relaxed sufficiently, particularly for larger sizes²⁸. Reducing the symmetry of the NPs can lift more selection rules for dipole transitions, opening new channels for photon absorption. This can be achieved by distorting the spherical shape toward rod-like (elongated in one dimension) or disc-like (elongated in two dimensions) shapes; NPs of such shapes have been already fabricated^{29–34} but only low-energy excitation spectra have been studied or analyzed in detail^{35–39}.

To illustrate our point, we selected two materials in which atomic coordination, the nature of bonds and the crystal lattice are all different, namely Si (with four-fold tetrahedral covalent bonds in the diamond lattice) and PbSe (with six-fold cubic ionic bonds in the rocksalt lattice). We considered NPs of these materials of various shapes, spherical, rod-like and disc-like, and approximately constant volume (corresponding to ~ 2 nm diameter for the spherical shape), and show thorough time-dependent density functional theory (TD-DFT) calculations of the optical absorption spectra that the lower-symmetry shapes (rods and discs) have higher absorption in the energy range E_g to $3E_g$, *independent* of their chemical composition and surface structure.

II. METHODOLOGY

We used the local-basis approach as implemented in the SIESTA code⁴⁰ and norm-conserving pseudopotentials⁴¹, with periodic cells in which the closest distance between surface atoms of the periodic images is larger than 1 nm; all structures were fully relaxed. For a check, we also performed plane-wave calculations with the VASP code⁴² and find excellent agreement between the results of the two different approaches. Absorption spectra were obtained from TD-DFT⁴³, with the generalized gradient PBE functional⁴⁴ in the exchange-correlation kernel. For relatively small NPs, TD-DFT provides a qualitatively correct description of excitation processes (unlike for the case of bulk solids) and is used here to discuss trends in excitation spectra Si and PbSe NPs as a function of their shape. The implementation of the TD-DFT method within SIESTA code was described in Refs. 45,46 in detail where this method applied both for molecules and small hydrogenated Si and Ge nanoclusters. In recent years other TD-DFT codes have been applied to hydrogenated Si and Ge nanoclusters (for example, Refs. 47–49 resulting very similar results to that with our implementation⁴⁶). In this study we apply the TD-DFT method for the well-known hydrogenated Si and the less-known PbSe nanoclusters. Spin-orbit interactions play an important role in PbSe due to the heavy Pb nuclei⁵⁰ and can significantly reduce the calculated fundamental gap of ~ 2 nm PbSe NPs⁵¹ but does not affect the geometry. Computationally it is prohibitive to calculate the TD-DFT excitation spectrum including spin-orbit coupling for relatively large nanoclusters while a simple DFT optical spectrum yields qualitatively wrong results. Thus, we calculated the excitation spectra of PbSe NPs without spin-orbit coupling and discuss below the error from this approximation.

We note here that TD-DFT method provides absorption spectrum with a semi-quantitative accuracy for semiconductor nanoclusters but does not yield the MEG efficiencies directly. It has been shown that impact ionization may explain the MEG, particularly, in PbSe nanoclusters^{52–55}. The calculation of impact ionization within perturbation approach needs the evaluation of about 2,000,000 Coulomb integrals between Kohn-Sham states in a relatively small $\text{Si}_{66}\text{H}_{64}$ nanocrystal for the appropriate energy range of biexciton generation. In addition, the dielectric function of this cluster has to be also determined accurately which is computationally demanding. It is technically now impossible to calculate the MEG fully *ab initio* for the sizes where the shape effects can be calculated by TD-DFT shown in this paper. Thus, we argue that if the intensity of absorption is larger so the MEG is larger as the available biexcitonic states grow quadratically with increasing number of available joint density of states while the single exciton states only linearly. Recent tight-binding calculations support this view⁵⁶. We notice that our recent full *ab initio* calculations on MEG also support our argument in small hydrogenated silicon nanoclusters⁵⁷.

III. RESULTS

We discuss first the Si NPs (Fig. 1). We built the spherical NP structure ($\text{Si}_{220}\text{H}_{144}$, labeled A1) under the constraint that it should exhibit T_d symmetry and every surface Si atom should be covalently bonded to at least two other Si atoms, with the dangling bonds passivated by H atoms. Hydrogenated Si NPs have been recently fabricated and it

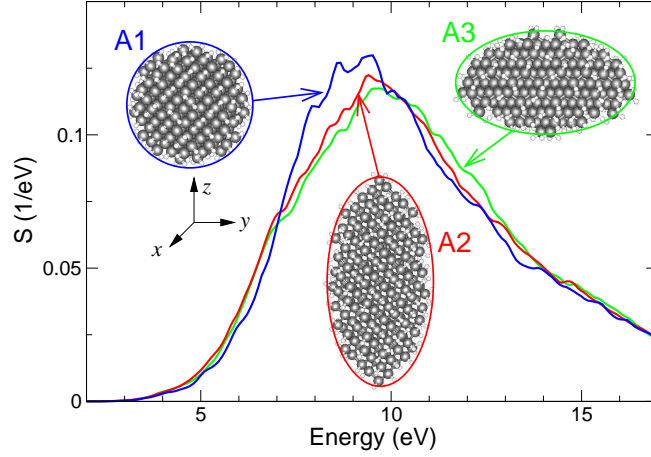


FIG. 1: (Color online) Optical absorption spectra of the Si NPs with spherical (A1), rod-like (A2) and disc-like (A3) shapes; the three atomic structures are shown as insets (Si atoms: grey spheres, H atoms: white spheres). The colored ellipses (circle for A1) show the approximate cross section on a plane containing one of the two equivalent directions (x, y) and the inequivalent direction (z) of the lower-symmetry A2 and A3 structures.

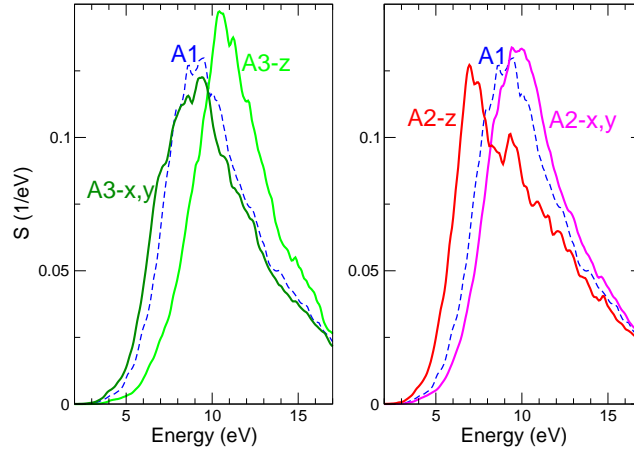


FIG. 2: (Color online) Polarization-resolved absorption spectra of the low-symmetry Si nanoparticles A2 and A3; axial directions are defined in Fig. 1. For comparison, the spectrum of A1 is also shown in dashed lines.

has been argued that these NPs are ideal for studying excitons experimentally⁵⁸. MEG in Si NPs was measured in a hexane solvent where the surface was presumably partially terminated by carbon-chains. The high energy excitation spectrum of Si NPs with carbon chains at the surface differs from the hydrogenated one⁵⁹, but including carbon-chain termination would increase the computational cost beyond what is currently feasible. Moreover, the *difference* in the calculated spectra of different shapes but with same surface termination, which is the key quantity of interest here, should be qualitatively similar for different surface terminations of Si NPs. We built the lower-symmetry rod-like ($\text{Si}_{219}\text{H}_{156}$, A2) structure and disc-like ($\text{Si}_{195}\text{H}_{148}$, A3) structure with constraints that their volumes should be almost equal to the volume of the spherical structure and the same surface constraints as in the spherical case. In the A2 structure the diameter along the z -direction is 2.8 nm and 1.7 nm along the ($x - y$) directions; the corresponding values for A3 are 1.0 nm and 2.4 nm.

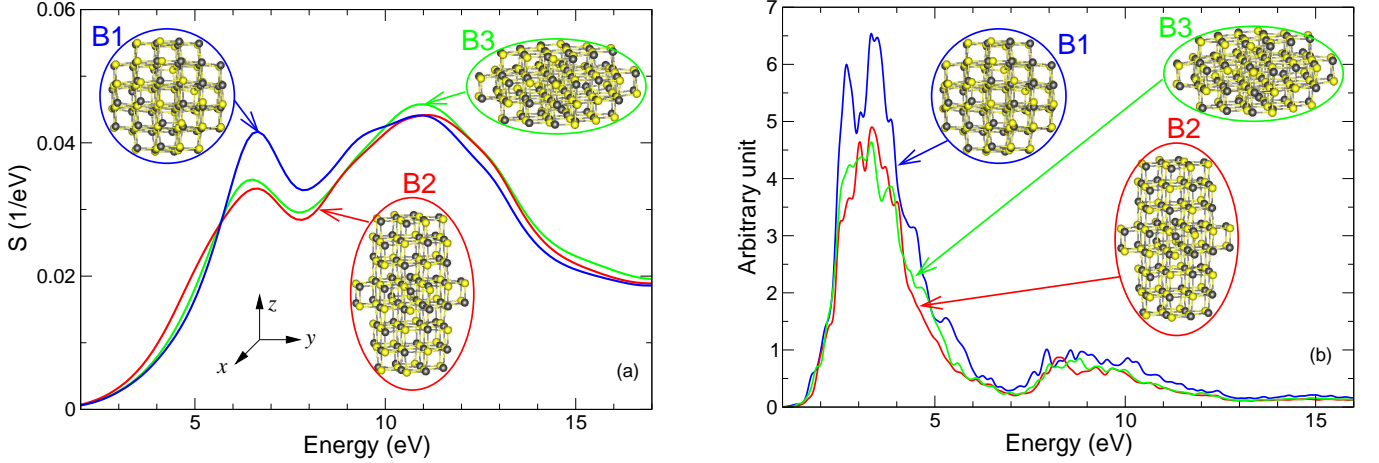


FIG. 3: (Color online) Optical absorption spectra of the PbSe NPs with spherical (B1), rod-like (B2) and disc-like (B3) shapes; the three atomic structures are shown as insets (Pb atoms: (grey) dark spheres, Se atoms: (yellow) light spheres). Other notation similar as in Fig. 1. (a) TD-DFT spectra, (b) DFT spectra

The calculated excitation spectra of Si NPs with different shapes are shown in Fig. 1. The absorption intensity is higher in rod- and disc-like shapes than in the spherical shape Si NPs, up to a characteristic energy of excitation above which the trend is opposite. For the NPs considered here, this characteristic energy is $\sim 3E_g$, demonstrating that the overall absorption can be increased in the E_g to $3E_g$ energy range relevant for PV applications. The rod- and disc-like shapes show very similar characteristics. The optical gap is the same within 0.08 eV for all the shapes (A1 : 2.12 eV, A2 : 2.06 eV, A3 : 2.14 eV) as expected since the deviation from the spherical shape is relatively small. The increase in the intensity of absorption in low-symmetry Si NPs can be partially explained by the relaxation of selection rules. An intuitive explanation is based on invoking quantum confinement effects: The NPs can be modeled by quantum boxes with infinitely large potential barriers; a simple analytical argument shows that the most symmetric quantum box (cube) has the lowest absorption compared to that of a general rectangular quantum box. In the case of low-symmetry NPs the low-lying energy states are less confined while the high-energy empty states are more confined along the short axes of NPs. This simple argument is actually borne out by our DFT calculations for the confinement of states in Si and PbSe NPs. By integrating the absorption spectrum in the E_g to $3E_g$ energy range we obtain an enhancement of about 25% for the rod-like shape (20% for the disc-like shape) relative to the spherical NP. These results indicate a larger number of exciton states in the rod-like and disc-like Si NP. In addition, E_{thr} might be reduced due to the lower symmetry of the system.

It is instructive to study the polarization dependence of the spectra for axially symmetric shapes in comparison to the spectrum of the spherical shape (see Fig. 2). The absorption is different along the z -direction and along the $(x-y)$ directions of the rod-like (red curve) and disc-like (green curve) Si NPs as expected from their symmetry. In the case of the rod-like Si NP the absorption is larger for light polarized along the z -direction than along the $(x-y)$ directions in the relevant energy region. A previous tight-binding study found this effect in Si nanoclusters⁶⁰. We explain this behavior by simple quantum confinement arguments as mentioned earlier: along the elongated z -axis the quantum confinement is considerably smaller than along the other axes. Thus, the electron states close to the gap are delocalized along the entire nanorod that can absorb z -polarized light with larger intensity. The states confined strictly across the nanorod ($x-y$ plane) are split by a much larger energy than the fundamental gap and consequently the absorption polarized along $(x-y)$ directions is more intense at higher energies. This simple explanation is in line with relative absorption intensities of a spherical NP versus a rod-like NP. In the disc-like NP, the quantum confinement is stronger along the z -direction than in the other directions, and the corresponding polarization dependence follows the pattern explained above: the absorption intensity is stronger at lower energies for light polarized along $(x-y)$ directions while the absorption intensity along the z -direction dominates at higher energies. These results suggest that proper orientation of the non-spherical NPs can lead to optimized absorption in PV devices.

We turn next to PbSe NPs, all with the same composition, $Pb_{68}Se_{68}$ (Fig. 3). We used the bond center as the origin to build the various structures, which automatically results in stoichiometric NPs with the full T_d symmetry retained for the spherical (B1) structure. The creation of a stoichiometric structure ensures that there are no artifacts

in the electronic structure such as deep gap states⁶¹. We followed a similar procedure to that employed for the Si NPs to construct stoichiometric rod-like (B2) and disc-like (B3) PbSe NPs. In the B2 structure the diameter along the z -direction is 2.2 nm while 1.6 nm along the $(x-y)$ directions; the corresponding values for B3 are 0.9 nm and 2.2 nm. Colloidal PbSe NPs exist in organic solvents (such as tetrachlorethylene) but there is no evidence from experiments or theory that covalent bonds are formed between the molecules of the solvent and the ionic PbSe particles. Thus, we did not use any surface passivation in PbSe NPs but allow the surface atoms to relax to find the minimum energy structure.

In bulk form, PbSe is very different from Si: it has much lower band gap, the rocksalt crystal structure, ionic bonds between the constituent atoms, and a non-reactive surface. Despite all of these differences the basic feature in the calculated absorption spectra of PbSe NPs [Fig. 3 (a)] are similar to those of the Si NPs. The absorption intensity is higher in rod- and disc-like shapes than in spherical shape PbSe NPs up to a characteristic energy of excitation, though the enhancement in absorption is more pronounced for rod-like than for disc-like PbSe NPs. In PbSe NPs we considered, this characteristic energy is well above $3E_g$ (it is close to $5E_g$), which shows that the overall absorption can be increased in the E_g to $3E_g$ energy range relevant to PV applications. The optical gap is the same within 0.2 eV for all the shapes (B1 : 1.25 eV; B2 : 1.13 eV; B3 : 1.33 eV). There is a dip in the calculated excitation spectra of PbSe NPs at very high energy, 7.5 eV, characteristic for all shapes. We attribute this dip to the energy gap between the valence Se p states and the Pb s states. While the energy gap between Pb s and Se p states may decrease by using more accurate methods, Pb s orbitals do not seem to play a role in absorption in the visible part of the solar cell spectrum. By integrating the absorption spectrum in the E_g $3E_g$ energy range for our PbSe NPs, we obtain an enhancement of about 31% for the rod-like (7% for the disc-like) PbSe NPs relative to the spherical shape. The increase in the absorption at low energy may be again explained by quantum confinement arguments similar to the case of Si NPs, though this effect is not as pronounced for PbSe NPs due to the hybridization of the bulk-like states with the surface states (see Fig. 4). The polarization dependence of the absorption spectra of PbSe NPs is very similar to that of Si NPs. The density of states of the PbSe NPs increases in the energy range about 1-2 eV below the highest occupied state in the rod-like and disc-like PbSe NPs relative to that of spherical PbSe NP. These states are associated with Se p orbitals and are localized on atoms along the elongated axis of the PbSe NPs; they contribute in the increase of absorption in the relevant energy range important for PV applications.

Finally, we comment on the error introduced by the neglect of spin-orbit coupling. Again, we emphasize that DFT provides qualitatively wrong excitation spectra giving a wrong shape of spectra as demonstrated in [Fig. 3, thus we choose to use TD-DFT but to neglect spin-orbit coupling in contrast to a previous work⁵¹. This coupling is effective on the Pb p -orbitals located in the “conduction band” (the unoccupied NP states) and would shift the calculated E_g to lower values, affecting the optical spectrum. We expect that the shape dependence of the spectrum will not change qualitatively, because the enhancement of absorption in the rod-like and disc-like shapes is mostly due to quantum confinement effects, which does not depend on the spin state but rather on the spatial localization of the wave functions. Moreover, as we discussed above, this quantum confinement will mostly change the density of states in the “valence band” associated with Se p orbitals where spin-orbit coupling is negligible.

IV. SUMMARY

In summary, we have investigated high energy excitations in Si and PbSe NPs using TD-DFT methods. We demonstrated that rod-like and disc-like nanoparticles show enhancement in absorption at energies of excitation where excitons and biexcitons can be created, relative to the absorption of spherical nanoparticles with the same volume. We also provided insight into the polarization dependence of the absorption of non-spherical nanoparticles. Shape manipulation of nanoparticles opens a route to maximize the overall absorption at a given volume and possibly to reduce the threshold energy for exciton generation. Our findings can help the design of nano-scale structures that exhibit enhanced MEG, which could prove useful for more efficient solar energy conversion.

Acknowledgement

AG acknowledges support from Hungarian OTKA No. K-67886, János Bolyai program from the Hungarian Academy of Sciences and NHDP TÁMOP-4.2.1/B-09/1/KMR-2010-0002 program. SM acknowledges partial financial supports

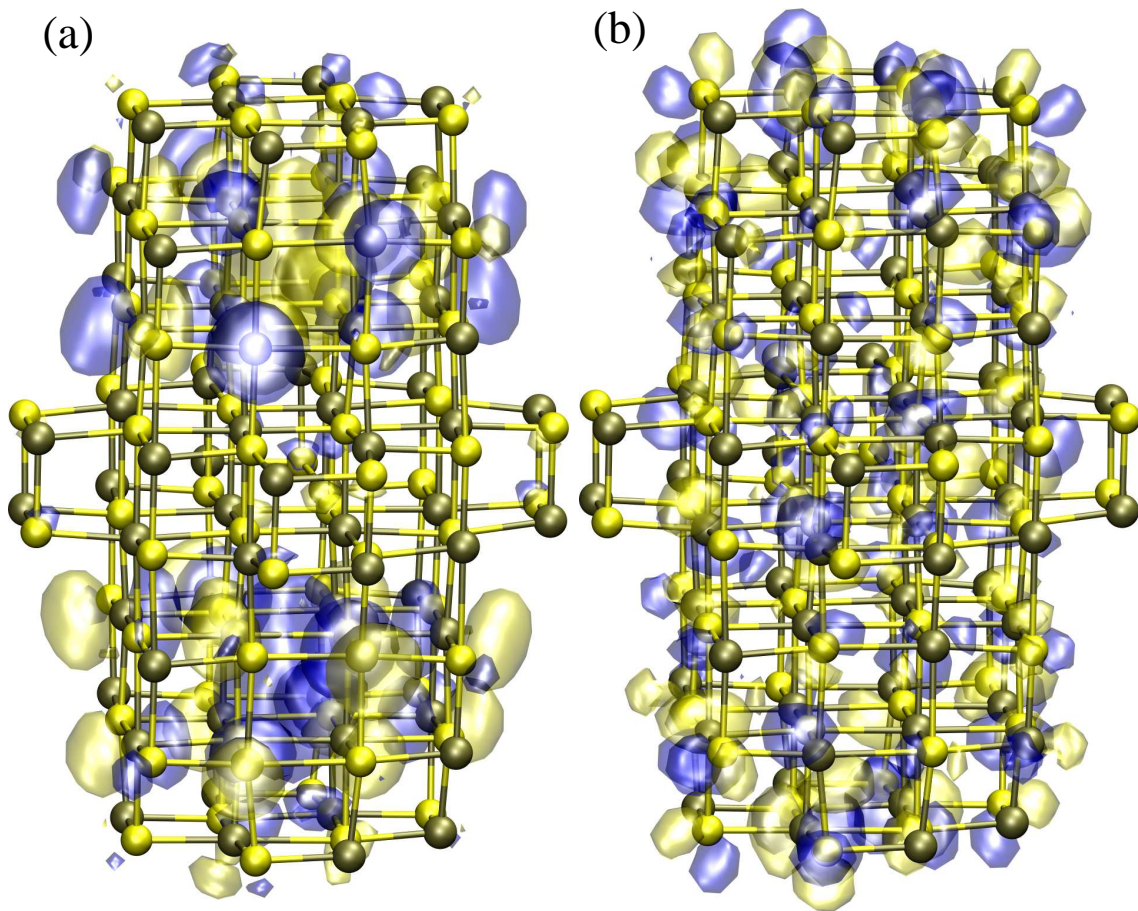


FIG. 4: (Color online) Selected wave functions of empty levels in rod-like PbSe NP (a) at low-end energy (E_g), (b) at high-end energy ($4E_g$) with respect to the highest occupied molecular orbital. Light (yellow) and dark (blue) lobes represent the isosurface of the positive and negative values of the selected wave functions, respectively. Pb atoms: (grey) dark spheres, Se atoms: (yellow) light spheres.

from hundred-talent program of CAS and NSFC (No. 11074287). GTZ acknowledges support by NSF-SOLAR 1035468.

* Electronic address: agali@eik.bme.hu

† Electronic address: smeng@iphy.ac.cn

- ¹ A. J. Nozik, *Physica E: Low-dimensional Systems and Nanostructures* **14**, 115 (2002).
- ² R. D. Schaller and V. I. Klimov, *Physical Review Letters* **92**, 186601 (2004).
- ³ R. J. Ellingson, M. C. Beard, J. C. Johnson, P. Yu, O. I. Micic, A. J. Nozik, A. Shabaev, and A. L. Efros, *Nano Letters* **5**, 865 (2005).
- ⁴ R. D. Schaller, V. M. Agranovitch, and V. I. Klimov, *Nature Physics* **1**, 189 (2005).
- ⁵ R. D. Schaller, M. A. Petruska, and V. I. Klimov, *Applied Physics Letters* **87**, 253102 (2005).
- ⁶ S. J. Kim, W. J. Kim, Y. Sahoo, A. N. Cartwright, and P. N. Prasad, *Applied Physics Letters* **92**, 031107 (2008).
- ⁷ R. D. Schaller, M. Sykora, S. Jeong, and V. I. Klimov, *The Journal of Physical Chemistry B* **110**, 25332 (2006), pMID: 17165979.
- ⁸ J. J. H. Pijpers, E. Hendry, M. T. W. Milder, R. Fanciulli, J. Savolainen, J. L. Herek, D. Vanmaekelbergh, S. Ruhman, D. Mocatta, D. Oron, A. Aharoni, U. Banin, and M. Bonn, *The Journal of Physical Chemistry C* **111**, 4146 (2007).
- ⁹ R. D. Schaller, J. M. Pietryga, and V. I. Klimov, *Nano Letters* **7**, 3469 (2007).
- ¹⁰ M. C. Beard, K. P. Knutsen, P. Yu, J. M. Luther, Q. Song, W. K. Metzger, R. J. Ellingson, and A. J. Nozik, *Nano Letters* **7**, 2506 (2007).
- ¹¹ G. Nair and M. G. Bawendi, *Physical Review B (Condensed Matter and Materials Physics)* **76**, 081304 (2007).
- ¹² J. J. H. Pijpers, E. Hendry, M. T. W. Milder, R. Fanciulli, J. Savolainen, J. L. Herek, D. Vanmaekelbergh, S. Ruhman, D. Mocatta, D. Oron, A. Aharoni, U. Banin, and M. Bonn, *The Journal of Physical Chemistry C* **112**, 4783 (2008).

- ¹³ M. Ben-Lulu, D. Mocatta, M. Bonn, U. Banin, and S. Ruhman, *Nano Letters* **8**, 1207 (2008).
- ¹⁴ M. T. Trinh, A. J. Houtepen, J. M. Schins, T. Hanrath, J. Piris, W. Knulst, A. P. L. M. Goossens, and L. D. A. Siebbeles, *Nano Letters* **8**, 1713 (2008).
- ¹⁵ G. Nair, S. M. Geyer, L.-Y. Chang, and M. G. Bawendi, *Physical Review B (Condensed Matter and Materials Physics)* **78**, 125325 (2008).
- ¹⁶ M. Ji, S. Park, S. T. Connor, T. Mokari, Y. Cui, and K. J. Gaffney, *Nano Letters* **9**, 1217 (2009).
- ¹⁷ J. J. H. Pijpers, R. Ulbricht, K. J. Tielrooij, A. Osherov, Y. Golan, C. Delerue, G. Allan, and M. Bonn, *Nature Physics* **5**, 811 (2005).
- ¹⁸ J. M. Luther, M. C. Beard, Q. Song, M. Law, R. J. Ellingson, and A. J. Nozik, *Nano Letters* **7**, 1779 (2007).
- ¹⁹ J. A. McGuire, J. Joo, J. M. Pietryga, R. D. Schaller, and V. I. Klimov, *Accounts of Chemical Research* **41**, 1810 (2008).
- ²⁰ G. I. Koleilat, L. Levina, H. Shukla, S. H. Myrskog, S. Hinds, A. G. Pattantyus-Abraham, and E. H. Sargent, *ACS Nano* **2**, 833 (2008).
- ²¹ M. C. Beard, A. G. Midgett, M. Law, O. E. Semonin, R. J. Ellingson, and A. J. Nozik, *Nano Letters* **9**, 836 (2009).
- ²² M. Sykora, A. Y. Koposov, J. A. McGuire, R. K. Schulze, O. Tretiak, J. M. Pietryga, and V. I. Klimov, *ACS Nano* **4**, 2021 (2010), pMID: 20369900.
- ²³ J. A. McGuire, M. Sykora, J. Joo, J. M. Pietryga, and V. I. Klimov, *Nano Letters* **10**, 2049 (2010), pMID: 20459066.
- ²⁴ W. A. Tisdale, K. J. Williams, B. A. Timp, D. J. Norris, E. S. Aydil, and X.-Y. Zhu, *Science* **328**, 1543 (2010).
- ²⁵ M. C. Beard, A. G. Midgett, M. C. Hanna, J. M. Luther, B. K. Hughes, and A. J. Nozik, *Nano Letters* **0**, (0).
- ²⁶ J.-W. Luo, A. Franceschetti, and A. Zunger, *Nano Letters* **8**, 3174 (2008).
- ²⁷ C. Delerue, G. Allan, J. J. H. Pijpers, and M. Bonn, *Phys. Rev. B* **81**, 125306 (2010).
- ²⁸ R. Koole, G. Allan, C. Delerue, A. Meijerink, D. Vanmaekelbergh, and A. Houtepen, *Small* **4**, 127 (2008).
- ²⁹ X. Peng, L. Manna, W. Yang, J. Wickham, E. Scher, A. Kadavanich, and A. P. Alivisatos, *Nature* **404**, 59 (2000).
- ³⁰ J. Hu, L.-s. Li, W. Yang, L. Manna, L.-w. Wang, and A. P. Alivisatos, *Science* **292**, 2060 (2001).
- ³¹ L.-s. Li, J. Hu, W. Yang, and A. P. Alivisatos, *Nano Letters* **1**, 349 (2001).
- ³² S. Kan, T. Mokari, E. Rothenberg, and U. Banin, *Nature Materials* **2**, 155 (2003).
- ³³ H. Yu, J. Li, R. A. Loomis, L.-W. Wang, and W. E. Buhro, *Nature Materials* **2**, 517 (2003).
- ³⁴ W.-k. Koh, A. C. Bartnik, F. W. Wise, and C. B. Murray, *Journal of the American Chemical Society* **132**, 3909 (2010), pMID: 20180556.
- ³⁵ T. Sadowski and R. Ramprasad, *Phys. Rev. B* **76**, 235310 (2007).
- ³⁶ Q. Zhao, P. A. Graf, W. B. Jones, A. Franceschetti, J. Li, Wang, and K. Kim, *Nano Letters* **7**, 3274 (2007).
- ³⁷ Y. Wang, R. Zhang, T. Frauenheim, and T. A. Niehaus, *The Journal of Physical Chemistry C* **113**, 12935 (2009).
- ³⁸ K. F. Karlsson, M. A. Dupertuis, D. Y. Oberli, E. Pelucchi, A. Rudra, P. O. Holtz, and E. Kapon, *Phys. Rev. B* **81**, 161307 (2010).
- ³⁹ N. Zonias, P. Lagoudakis, and C.-K. Skylaris, *Journal of Physics: Condensed Matter* **22**, 025303 (2010).
- ⁴⁰ J. M. Soler, E. Artacho, J. D. Gale, A. García, J. Junquera, P. Ordejón, and D. Sánchez-Portal, *Journal of Physics: Condensed Matter* **14**, 2745 (2002).
- ⁴¹ N. Troullier and J. L. Martins, *Phys. Rev. B* **43**, 1993 (1991).
- ⁴² G. Kresse and J. Furthmüller, *Phys. Rev. B* **54**, 11169 (1996).
- ⁴³ S. Meng and E. Kaxiras, *The Journal of Chemical Physics* **129**, 054110 (2008).
- ⁴⁴ J. P. Perdew, K. Burke, and M. Ernzerhof, *Phys. Rev. Lett.* **77**, 3865 (1996).
- ⁴⁵ A. Tsolakidis, D. Sánchez-Portal, and R. M. Martin, *Phys. Rev. B* **66**, 235416 (2002).
- ⁴⁶ A. Tsolakidis and R. M. Martin, *Phys. Rev. B* **71**, 125319 (2005).
- ⁴⁷ G. Neshet, L. Kronik, and J. R. Chelikowsky, *Phys. Rev. B* **71**, 035344 (2005).
- ⁴⁸ Walker, B. G., Hendy, S. C., Gebauer, R., and Tilley, R. D., *Eur. Phys. J. B* **66**, 7 (2008).
- ⁴⁹ T. J. Pennycook, G. Hadjisavvas, J. C. Idrobo, P. C. Kelires, and S. T. Pantelides, *Phys. Rev. B* **82**, 125310 (2010).
- ⁵⁰ S.-H. Wei and A. Zunger, *Phys. Rev. B* **55**, 13605 (1997).
- ⁵¹ R. Leitsmann and F. Bechstedt, *ACS Nano* **3**, 3505 (2009), pMID: 19873980.
- ⁵² A. Franceschetti, J. M. An, and A. Zunger, *Nano Letters* **6**, 2191 (2006).
- ⁵³ G. Allan and C. Delerue, *Phys. Rev. B* **73**, 205423 (2006).
- ⁵⁴ E. Rabani and R. Baer, *Nano Letters* **8**, 4488 (2008).
- ⁵⁵ C. Sevik and C. Bulutay, *Phys. Rev. B* **77**, 125414 (2008).
- ⁵⁶ G. Allan and C. Delerue, *Phys. Rev. B* **77**, 125340 (2008).
- ⁵⁷ M. Vörös, A. Gali, D. Rocca, G. Zimanyi, and G. Galli, *Ab initio theory of impact ionization applied to silicon nanocrystals*, American Physical Society March Meeting, Talk P41.5, 2011.
- ⁵⁸ B. Goller, S. Polisski, H. Wiggers, and D. Kovalev, *Applied Physics Letters* **97**, 041110 (2010).
- ⁵⁹ A. Gali, M. Vörös, D. Rocca, G. T. Zimanyi, and G. Galli, *Nano Letters* **9**, 3780 (2009), pMID: 19785388.
- ⁶⁰ F. Trani, G. Cantele, D. Ninno, and G. Iadonisi, *Phys. Rev. B* **72**, 075423 (2005).
- ⁶¹ A. Franceschetti, *Physical Review B* **78**, 075418 (2008).